RL-TR-95-144
In-House Report
June 1995

EFFECTIVE NON-LINEAR REFRACTIVE INDEX OF VARIOUS OPTICAL MATERIALS

John Malowicki

APPROVED FOR PUBLIC RELEASE; DISTRIBUTION UNLIMITED.

Rome Laboratory
Air Force Materiel Command
Griffiss Air Force Base, New York

This report has been reviewed by the Rome Laboratory Public Affairs Office (PA) and is releasable to the National Technical Information Service (NTIS). At NTIS it will be releasable to the general public, including foreign nations.

RL-TR-95-144 has been reviewed and is approved for publication.

APPROVED:

JAMES W. CUSACK, Chief
Photonics Division
Surveillance & Photonics Directorate

FOR THE COMMANDER:

DONALD W. HANSON
Director of Surveillance & Photonics

If your address has changed or if you wish to be removed from the Rome Laboratory mailing list, or if the addressee is no longer employed by your organization, please notify RL (OCPC) Griffiss AFB NY 13441. This will assist us in maintaining a current mailing list.

Do not return copies of this report unless contractual obligations or notices on a specific document require that it be returned.

REPORT DOCUMENTATION PAGE

Form Approved
OMB No. 0704-0188

1. AGENCY USE ONLY (Leave Blank)	2. REPORT DATE	3. REPORT TYPE AND DATES COVERED
	June 1995	In-House Jan 94 - Mar 95

4. TITLE AND SUBTITLE
EFFECTIVE NON-LINEAR REFRACTIVE INDEX OF VARIOUS OPTICAL MATERIALS

5. FUNDING NUMBERS
PR-4600
TA-PS
WU-YS

6. AUTHOR(S)
John Malowicki

7. PERFORMING ORGANIZATION NAME(S) AND ADDRESS(ES)
Rome Laboratory (OCPC)
25 Electronic Parkway
Griffiss AFB NY 13441-4515

8. PERFORMING ORGANIZATION REPORT NUMBER
RL-TR-95-144

9. SPONSORING/MONITORING AGENCY NAME(S) AND ADDRESS(ES)
Rome Laboratory (OCPC)
25 Electronic Parkway
Griffiss AFB NY 13441-4515

10. SPONSORING/MONITORING AGENCY REPORT NUMBER

11. SUPPLEMENTARY NOTES
Rome Laboratory Project Engineer: John Malowicki/OCPC (315)330-3146

12a. DISTRIBUTION/AVAILABILITY STATEMENT
Approved for public release; distribution unlimited.

12b. DISTRIBUTION CODE

13. ABSTRACT (Maximum 200 words)

Photo-induced effective nonlinearity, n_2, of BSO crystal is measured by using a Z-scan method which is based on the self-focusing/defocusing effect. The Z-scan technique is a simple yet accurate way to measure n_2. An optical limiter utilizing photo-induced lensing is investigated and the influence of spatial self-phase modulation for strong CW illumination is presented.

14. SUBJECT TERMS
Z-scan, BSO, KNSBN, Effective Nonlinearity, n_2 Spatial Self-phase Modulation, Optical Limiting

15. NUMBER OF PAGES
40

16. PRICE CODE

17. SECURITY CLASSIFICATION OF REPORT	18. SECURITY CLASSIFICATION OF THIS PAGE	19. SECURITY CLASSIFICATION OF ABSTRACT	20. LIMITATION OF ABSTRACT
UNCLASSIFIED	UNCLASSIFIED	UNCLASSIFIED	UL

Table of Contents

List of Figures

List of Tables

List of Symbols

a	correction factor for geometrical and wave optics derived equations
α	linear absorption coefficient
d	distance between the focal plane in free space and the aperture plane
f	an empirical constant defined as $f = 0.406(1-s)^{0.25}$
h	thickness of the crystal
I_ω	intensity at the Gaussian beam waist inside the sample
$I_\omega(r)$	Gaussian illumination profile
k_z	wave vector of the incident radiation
ℓ_e	effective optical thickness
λ	wavelength of the laser
n_o	inherent index of the crystal
Δn	light induced refractive index change
n_2	effective non-linear refractive index
P_a	power before limiting aperture
P_T	power transmitted by limiting aperture
ΔP_{p-v}	difference between the peak and valley of the position dispersion curve
$\Phi(r)$	radially varying phase
$\Delta\Phi_0$	on axis nonlinear phase shift
ϕ_0	uniform retardation due to the n_0 of the crystal
r_a	radius of limiting aperture
s	aperture transmittance
T	normalized transmittance of the limiting aperture
ω_a	radius of beam at limiting aperture
ω_o	radius of beam at focus
z	distance between the focal plane in free space and the center of the sample
z_{dl}	diffraction length of focusing lens
z_0	focal plane of the lens

Acknowledgments

The author would like to thank Dr. Song for his help and encouragement, Serey Thai for his help in conducting this research, and Doug Norton for his help in writing macros in MacPhase. Without their support this paper would not be possible.

1. Introduction

This paper will detail the research done on the non-linear refractive index of various optical materials, specifically, Bismuth Silicon Oxide (BSO), and a Ce-doped $Ba_{2-x}Sr_xK_{1-y}Na_yNb_5O_{15}$ (KNSBN:Ce) crystal. The areas presented are the use of the Z-scan technique to measure the non-linear refractive index of the crystals, use of the samples as optical limiters, investigation into the self phase modulation inherent to the samples, and experimental results for each of the areas. Recently, the self focusing in new optical materials such as KNSBN:Ce and bacteriorhodopsin (BR) under low CW HeNe illumination were reported[1,2]. In this paper, the properties of the BSO and KNSBN:Ce crystals were investigated using a high power Argon-Ion laser.

The major property of interest is that of the non-linear refractive index of the crystals. Because of this nonlinear refractive index, a Gaussian beam propagating through the crystals induces a lens-like refractive index profile. This refractive index change in turn modifies the beam propagation. It is important to understand this lensing effect in order to better use the material in optical system applications.

The Z-scan technique offers a non-complicated yet precise method of measuring the effective non-linear refractive index coefficient of the samples. All that is needed is the laser, a focusing lens, an aperture, and a power meter. This method is based on the self-focusing or defocusing phenomena that occurs as the sample is translated through the focus of the lens in the direction of propagation, or the Z direction.

After the measured and derived results are presented, the use of the samples as an optical limiter is investigated. The optical configuration is the same except that the crystal is stationary while the power is increased. An aperture is used in conjunction with the self-focusing or defocusing effect of the crystal to limit the amount of power transmitted down the optical path.

Finally the effect of self phase modulation on the samples is investigated. Self phase modulation occurs along with self focusing/defocusing and has an important influence on the optical limiting behavior of the crystals. A comparison between experimental and measured data is also presented.

2. Z-Scan Theory

The Z-scan is a sensitive and convenient method for measuring the light induced changes in the effective nonlinear refractive index and absorption coefficient of optical

materials[3,4]. The Z-scan is based on the transformation of the phase distortion associated with the self-lensing into an amplitude distortions during the beam propagation.

The experimental arrangement is shown in Fig 1. A lens is used to focus the illuminating laser as the crystal is translated along the optical path (the Z-scan). A focusing lens is used to suppress the beam fanning effect of photorefractive materials, which is proportional to the beam's lateral dimension, and to make the self focusing the dominant effect. In particular, KNSBN has a strong fanning effect even under low illumination intensities[5]. A limiting aperture is placed past the focus of the lens and a detector is used to measure the output intensity. The aperture is set to let only half the light intensity pass when no crystal is in the path. The aperture's intensity transmittance, s, is defined as the ratio of output power to input laser beam power. The crystal is placed directly behind the lens and translated through focus. The defocusing (focusing) of the crystal will allow more (or less) of the light to pass the aperture by creating a longer (or shorter) effective focal length of the lens and crystal system. The beam diameter at the aperture is compressed or expanded with this changing effective focal length. Measurements of the intensity at the detector with respect to crystal position give the position dispersion curves which can be used to find the sign and magnitude of the focusing. A pre-focal transmittance minimum (valley), followed by a post-focal transmittance maximum (peak) indicates a positive lensing. Fig. 1 shows the case of positive dispersion, with less then more light transmitted by the aperture as the sample is translated through focus.

It is believed that the focusing effect in KNSBN and BSO is due mainly to thermal effects of the incident radiation on the index of refraction of the crystal[1]. The intensity dependence of the refractive index can be written as $n = n_o + \Delta n = n_o + n_2 I_\omega$ where n_o is the index of the crystal, Δn is the light induced index change, and n_2 is the effective non-linear refractive index. The magnitude of n_2 can be determined from[3]

$$n_2 = \frac{\lambda \Delta P_{p-v}}{2\pi I_\omega f}\left(\frac{\alpha}{1-e^{-\alpha h}}\right) \qquad (1)$$

where ΔP_{p-v} is the difference between the peak and valley of the position dispersion curve, α is the linear absorption coefficient, h is the thickness of the sample, f is an empirical constant defined as $f = 0.406(1-s)^{0.25}$ where s is the aperture linear transmittance, and I_ω is the intensity at the Gaussian beam waist inside the sample

calculated by $I_\omega = 2P / \pi\omega^2$. Here P is the laser power and ω is the waist radius of the illumination beam in the crystal.

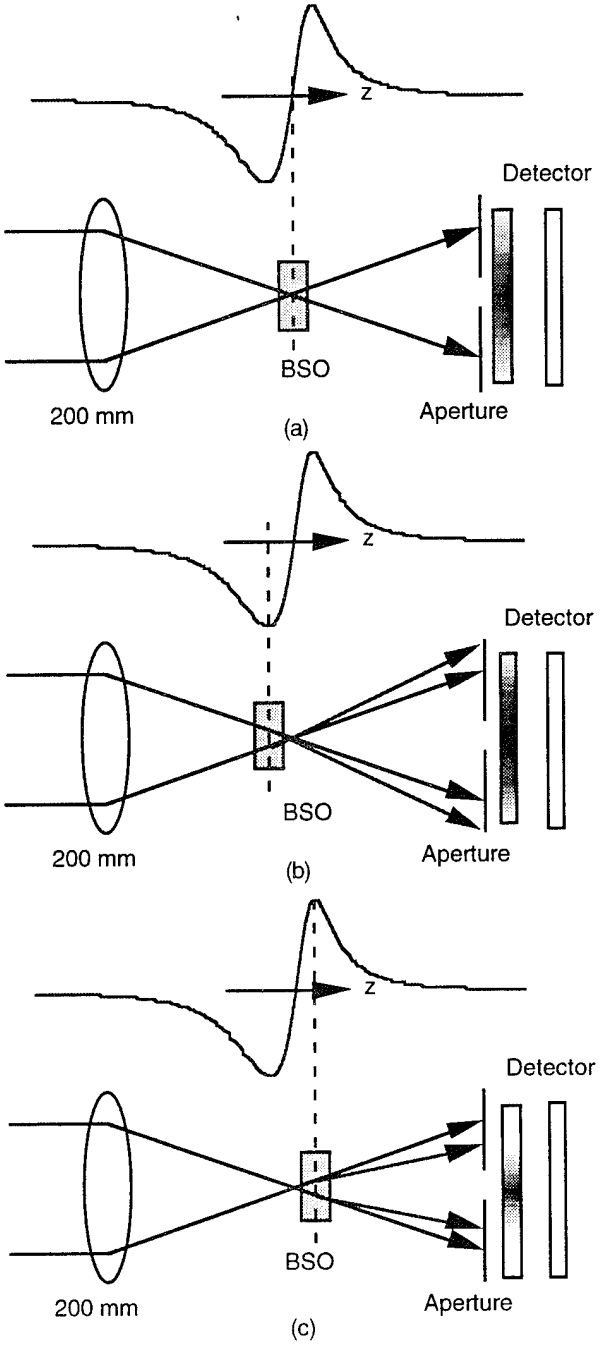

Fig. 1 Experimental setup for Z-scan measurement.

The Z-scan can be calculated[6] by knowing that the power transmitted through the aperture of radius r_a is given by

$$P_T(z) = P_a\left[1 - \exp(-\frac{2r_a^2}{\omega_a^2})\right] \qquad (2)$$

where ω_a is the beam radius at the aperture and P_a is the power at the aperture. If the power fluctuates with time, the transmitted power is given by[6]

$$T(z) = \frac{\int_0^\infty P_T(z,t)dt}{s\int_0^\infty P_a(t)dt} \qquad (3)$$

where s is the aperture transmittance. If temporal variations can be ignored, the above equation can be rewritten as[6]

$$T(z) = \frac{1 - \exp(-\frac{2r_a^2}{\omega_a^2})}{s} \qquad (4)$$

where ω_a is given by[6]

$$\frac{\omega_a^2}{\omega_0^2} = D^2\left(1 - \frac{2\Delta\Phi_0(D-x)x}{aD(1+x^2)^2}\right) + \left(1 - \frac{2\Delta\Phi_0(D-x)}{a(1+x^2)^2}\right) \qquad (5)$$

where $\Delta\Phi_0$ is the on axis nonlinear phase shift, $D=d/z_0$ and $x= z/z_0$ and a is a correction factor which a suitable choice for is $a \cong 6.4(1-s)^{0.35}$. Fig. 2 shows the calculated curve for the Z-scan transmittance compared to the actual data for KNSBN at 488nm.

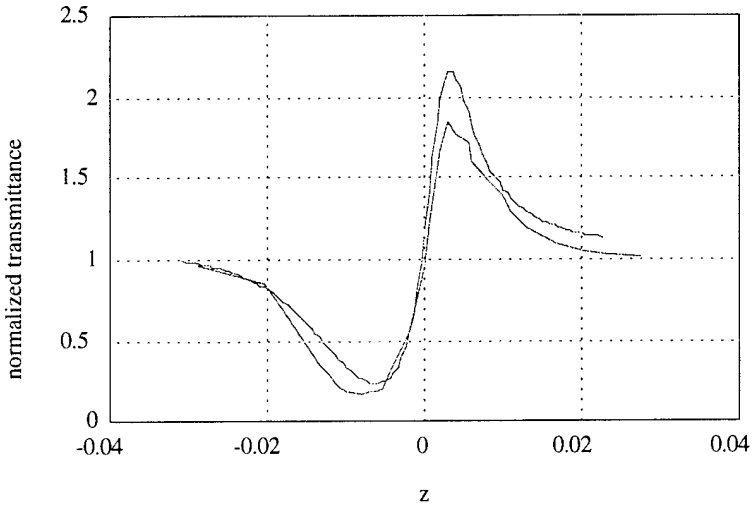

Fig. 2 Z-scan for KNSBN at 488nm, a : calculated, b : measured.

The Z-scan theory presented here assumes the crystal can be treated as a thin sample when its thickness is less than the diffraction length of the focusing lens. The diffraction length, z_{dl}, is:

$$z_{dl} = \frac{\pi\omega^2}{\lambda} \tag{6}$$

Taking the data in the experiment using BSO, ω is 32μm, n is 2.6, and λ is 514.5nm, the value of z_{dl} is approximately 14mm. The BSO crystal thickness is 4mm so it can indeed be treated as a thin sample.

When the length of the crystal is on the order of, or greater than z_{dl}, the Z-scan in Fig. 3 can be expected[3,6]. The peaks and valleys of the Z-scan trace have become more pronounced and further separated. A conceptual understanding can be obtained if the flattened transmittance curve about z_0 is considered first. When the thick sample is centered at z_0, the crystal will create large local phase distortions in the beam, but the prefocal distortion will be balanced out by the postfocal distortion. It can be thought of as two lenses centered about z_0 with the second lens canceling the effect of the first lens. Therefore, the far field pattern will be relatively unchanged giving a flat transmission line.

As for the peak and valley, the maximum and minimum occur when the focus is at the surfaces of the sample. Take the case of positive n_2. When the focus is at the back face of the sample, all of the lensing is acting to decrease the system focal length leading to a minimum in the transmission curve. As the sample begins to move through focus, the competing effects of the prefocal and postfocal phase distortions start to cancel each

other, leading to the flattened curve. The opposite happens after focus when the focal point is at the front surface of the crystal and all the lensing tends to focus the beam, allowing more light to pass the aperture leading to a maximum in transmittance.

For the thin sample, the peak and valley are separated by approximately $1.7\,z_{dl}$. For the thick sample, since the thickness is now on the order of, or greater than, the diffraction length z_{dl}, the thickness dominates and begins to push the peak and valley apart. The peak and valley occur when the focus is at either the front or back surface. The solid line in Fig. 3 is for the case of positive n_2, and the dashed line is for negative n_2.

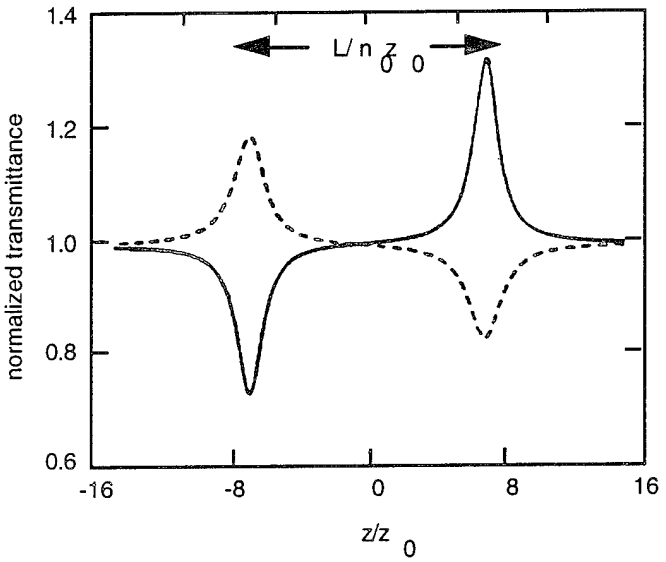

Fig. 3 Position dispersion curves for a Z-scan of a thick sample.

3. Z-scan experimental results

Position dispersion curves for a sample of BSO are shown below in Fig. 4. These position dispersion curves can be used to obtain a value of n_2 for BSO. Each of the curves correspond to a different input power level which is the reason for the different amplitudes of the curves. Note that in Eq. 1, n_2 is related to the difference in peak and valley divided by the input intensity so that each position dispersion curve should yield similar values of n_2. From these curves, the average n_2 was found to be $1.47 \times 10^{-6}\text{cm}^2/\text{W}$. This is comparable with the $n_2 = 1.9 \times 10^{-6}\text{cm}^2/\text{W}$ reported in Ref. 7.

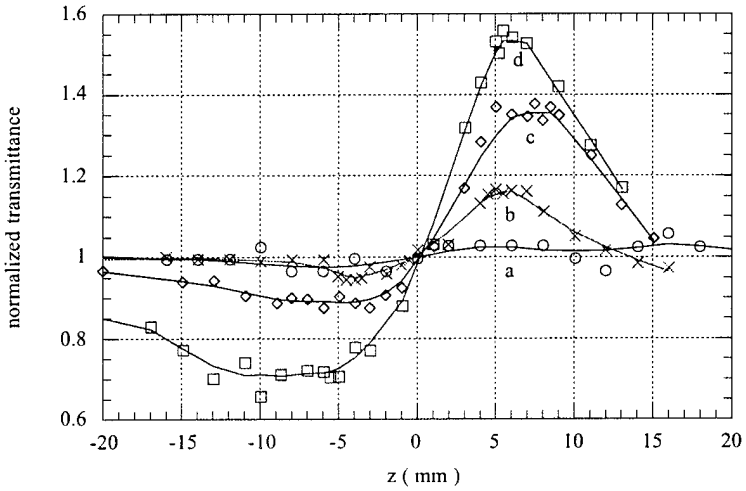

Fig. 4 Position dispersion for the BSO crystal for powers: curve a, 0.1 mW; b, 1 mW; c, 5 mW and d, 10 mW.

For the KNSBN:Fe crystal, position dispersion curves are presented in the Fig. 5. The figures are for 514.5nm, 488nm, and 476nm. It is noted that the magnitude of the curves varies with the polarization of the incident illumination. The polarizations were parallel and perpendicular to the C-axis of the crystal. This can be explained by a difference in the absorption coefficients of KNSBN for orthogonal polarizations[1]. The absorption affects the change in the index of refraction leading to a larger or slightly smaller position dispersion curves. In other words, the less absorption the crystal has, the smaller the change in the index of refraction Δn, leading to a smaller variation in the peak and valley of the position dispersion curve. For the opposite case of higher absorption, the position dispersion curve would naturally exhibit a greater variation in the peak to valley. Table 1 below gives the values of the absorption for the two polarizations at the wavelengths used. The n_2 for KNSBN is positive. Note that this is different from $KNbO_3$ where the light induced lensing is negative[9,10]. Also a definite difference can be seen in the absorption coefficients for the different polarizations.

λ (nm)	514.5	514.5	488	488	476	476
polarization	o	e	o	e	o	e
index	2.36	2.295	2.38	2.316	2.4	2.324
Power (mW)	22.3	22.7	22.3	23	22.3	23
%R	0.1638	0.1595	0.1667	0.1575	0.1696	0.1587
%T	0.09025	0.06875	0.062	0.048	0.05	0.037
α (cm^{-1})	4.0948	4.6832	4.8318	5.3876	5.2481	5.9024
ω (μm)	34	34	32	32	30	30
I (W/cm^2)	1228.1	1250.1	1386.4	1429.9	1577.4	1626.9
ΔP_{p-v}	1.15	1.45	1	1.45	1.2	1.6
L_e	0.2127	0.193	0.1885	0.1731	0.1767	0.1606
n_2 (cm^2/W)	1.06×10^{-7}	1.31×10^{-7}	0.77×10^{-7}	1.08×10^{-7}	0.79×10^{-7}	1.03×10^{-7}

Table 1 Results of KNSBN at 514.5nm, 488nm, and 476nm.

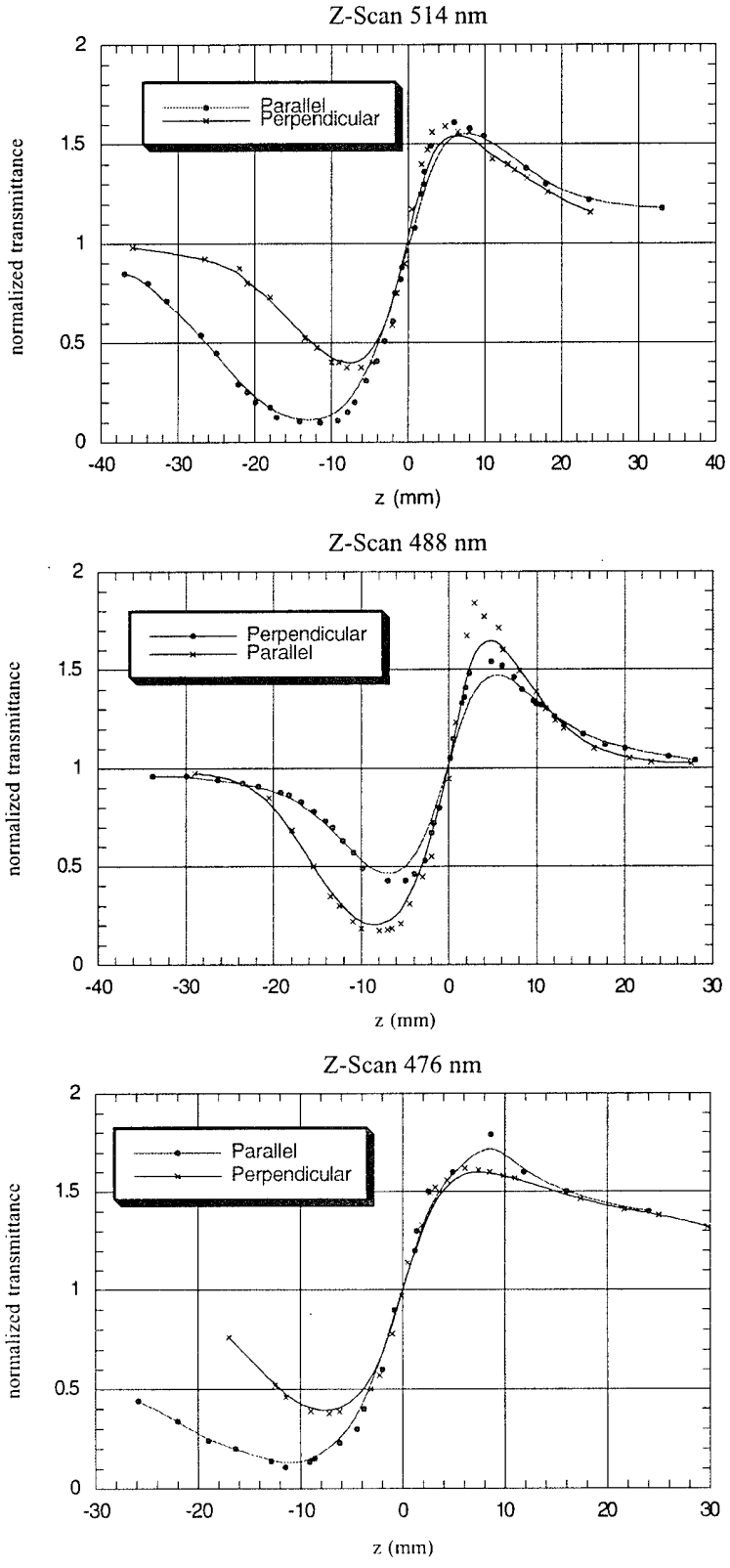

Fig. 5 Z-scan results for KNSBN showing the effects of polarization

4. Optical Limiting

An optical limiter is a device which produces an output power that is decreasingly proportional to the input power when the input is beyond a certain threshold value. It has many applications in laser damage protection. The self-focusing nature of KNSBN and BSO can be used to limit the optical intensity transmitted through a system[2,6,8]. By using a lens and an aperture as shown in Fig. 1, and placing the crystal in the valley of the position dispersion curve, the intensity transmitted is not allowed to increase linearly but is limited[5]. As the laser power is increased, the intensity measured before the aperture is taken to be the input power and the intensity past the aperture is the output power. The plot of output vs input power shows the nature of the crystal optical limiting. The optical limiting experiment was repeated for various apertures; it was found that the value of s around 0.5 produces the best optical limiting curve, i.e. the output is very flat. This experimental data supports selection of s to be 0.5 in the Z-scan experiment. Fig. 6 shows various optical limiting curves for the BSO crystal.

For KNSBN, the limiting was measured at three Argon wavelengths, 514nm, 488nm, and 476nm. It can be seen in Figs. 7 and 8 that the optical limiting is strongly wavelength dependent. This is most likely explained by an absorption wavelength dependence. A characteristic dip in the transmitted intensity is evident at 30mw. This oscillation can perhaps be best explained by self phase modulation of the incident beam.

5. Optical Limiting experimental results

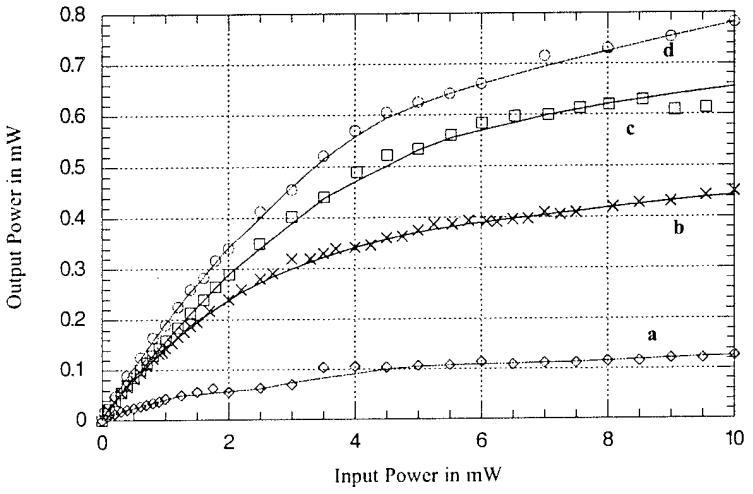

Fig. 6 Behavior of BSO optical limiting for various aperture's linear intensity transmittance: curves a, b, c and d are for s values of 0.2, 0.5, 0.66 and 0.8 respectively.

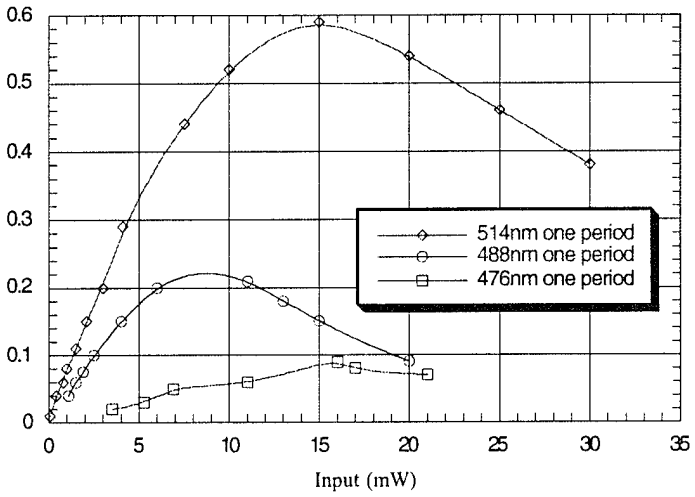

Fig. 7 Optical limiting for KNSBN for 514nm, 488nm and 476nm up to first dip.

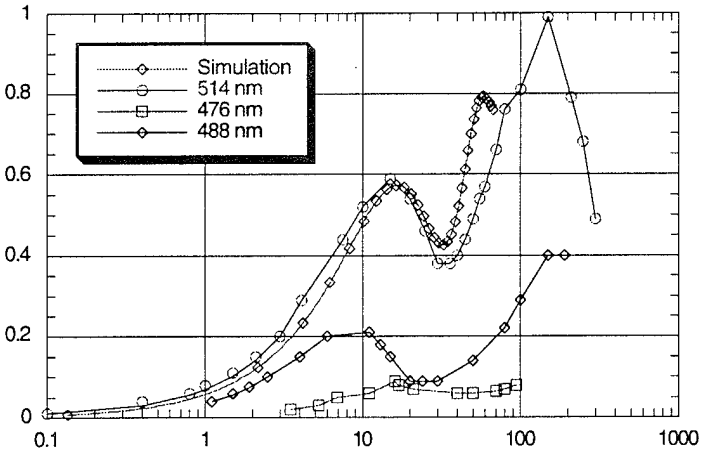

Fig. 8 Optical limiting for KNSBN for 514nm, 488nm and 476nm at higher powers and simulation data.

6. Self Phase Modulation

Self phase modulation (SPM) occurs in conjunction with self focusing. SPM is an intensity dependent effect and is related to the non-linear coefficient n_2. As the beam propagates through the crystal, the intensity distribution of the beam affects the index of the crystal which in turn affects the propagation of the beam. The change in the index of refraction not only has a focusing effect on the beam but also causes a phase change in the beam as well. The crystal will appear to have a different thickness corresponding to the

change in the index of refraction. In the context of self focusing, the Gaussian beam profile of the incident radiation leads to a varying phase change across the beam profile given by

$$\Phi(r) = \frac{2\pi \ell_e n_2}{\lambda} I_\omega(r) \tag{7}$$

where $I_\omega(r)$ is the Gaussian illumination profile and ℓ_e is the effective optical thickness defined as

$$\ell_e = \frac{1 - e^{-\alpha \ell}}{\alpha} \tag{8}$$

where α is the effective absorption coefficient.

As the intensity increases to the point that the phase change exceeds 2π, the far-field pattern begins to exhibit a concentric ring pattern. More rings become apparent as the phase continues through multiple 2π phase shifts. The total number of rings N can be estimated by a following relationship,

$$N = \frac{\Phi_{\max}}{2\pi} = \frac{n_2 I_\omega \ell_e}{\lambda} \tag{9}$$

The far field projection of this complex intensity distribution can be calculated by assuming the input intensity is Gaussian and by using the phase shift expressed in Eq. 7. The field amplitude at the exit surface of the crystal can be expressed as[11]

$$E(r) = [I_\omega(r)]^{1/2} \exp\{i[k_z z + \Phi(r) + \phi_0]\} \tag{10}$$

where $\Phi(r)$ is the phase shift from Eq. 7 and ϕ_0 is the uniform retardation due to the n_0 of the crystal. Simply by taking the Fourier transform of the above equation, the far-field radiation pattern can be obtained.

As the intensity of the irradiation increases, the phase change becomes stronger which varies the interference pattern. When the pattern goes through a minimum at the center of the beam, the effective transmittance of the system is lessened. The oscillatory nature of the phase change with intensity explains the oscillations in the plots of the output power.

A simulation of the above theory was done using MatLab and the results were consistent with the observed experimental results. Appendix B contains the MatLab code along with plots of the intensity profile and optical limiting curve. Fig. 8 shown above, contains a comparison of the calculated and measured optical limiting curves for the case of KNSBN at 514nm.

7. Self Phase Modulation Experimental Results

Fig. 9 shows line scan plots of the far-field intensity pattern resulting from the self phase modulation of a BSO crystal. Note that the powers used in this figure are much higher than that of the optical limiting curves in Fig. 6, which explains why no oscillations in the optical limiting curves are apparent. Fig. 10 shows the predicted intensity profiles resulting from self phase modulation.

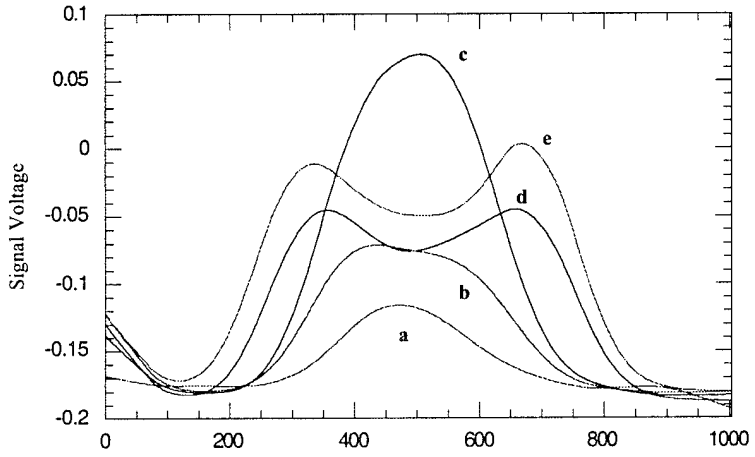

Fig. 9 Transverse intensity profiles of transmitted beam.
Curves a, b, c, d and e are for 5, 53, 66, 136, 156 mW respectively.

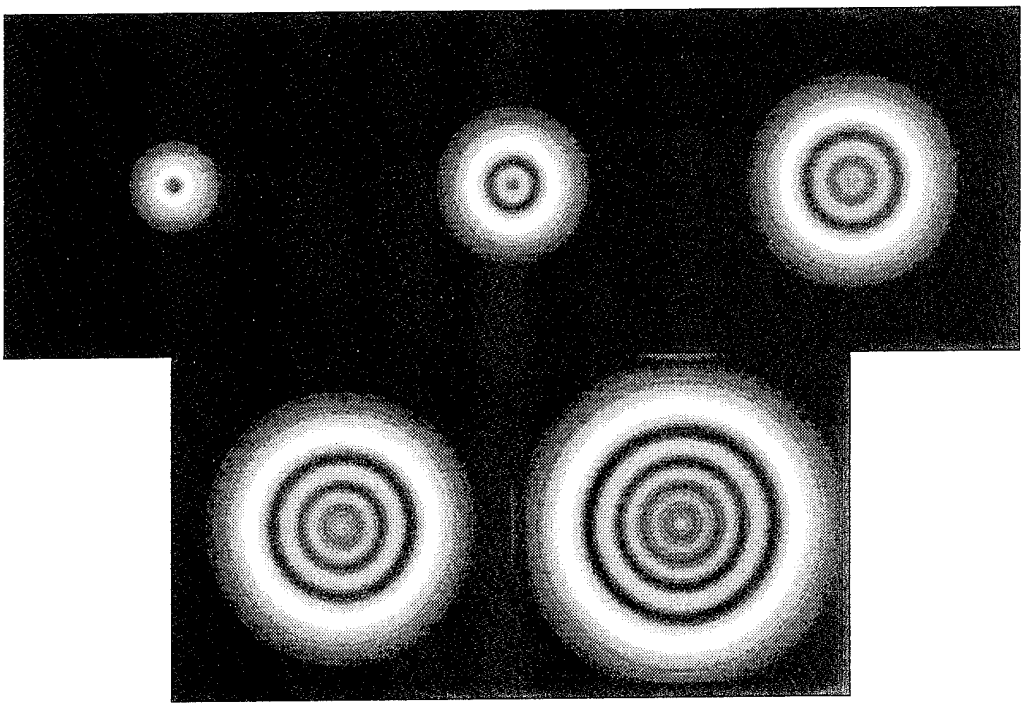

Fig. 10 Results of calculations for the beam profile due to self phase modulation.

The results in Fig. 11 were obtained with a Sony XC-75 black and white camera and a Spiricon beam profiler which was used to transfer the pictures via GPIB to an Apple Mac IIcx. The pictures clearly show the ring structure which results from the phase distortion of the crystal. These results were from a BSO crystal.

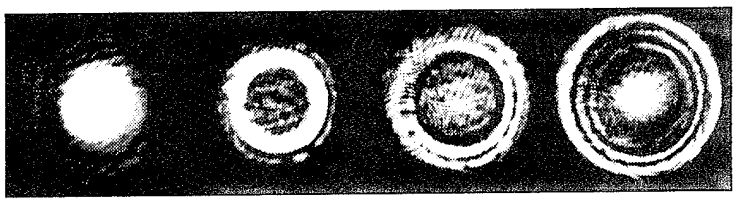

Fig. 11 Far-field ring patterns for incident intensities: 150mW, 302mW, 378mW, and 514mW.

8. Conclusion

The experimental method for the measurement of the non-linear refractive index of BSO and KNSBN has been presented along with the measured results. For BSO it was found that n_2 is on the order of 10^{-6} cm^2/W. This result is consistent with previously reported results based on the interferometric method. For KNSBN it was on the order of 10^{-7} cm^2/W. The use of these materials as optical limiters has been investigated along with the best configuration for their use. In the case of BSO, it was shown that its performance as a limiter is at optimum when the aperture's linear transmission s is set to 0.5. Both crystals pointed out that for higher input power the self phase modulation effect could not be ignored. The self-phase effect leads to a concentric ring pattern in the far-field when the maximum phase distortion exceeds 2π. This ring pattern has a profound effect on the optical limiting curve. Calculated optical limiting curves for self phase modulation were in agreement with measured data.

References

1. Q. W. Song, C. Zhang, P. Talbot, H. Chen, and X. Liu, "Self-focusing in KNSBN:Ce crystal under low power HeNe laser illumination," Opt. Mat., Vol. 2, pp. 59-64, 1993.
2. Q. W. Song, C. Zhang, R. Gross, and R. Birge, "Optical limiting by chemically enhanced bacteriorhodopsin films," Opt. Lett., Vol 18, No. 10, pp. 775-777, May 1993.
3. M. Sheik-Bahae, A. A. Said, T. H. Wei, D. J. Hagan, M. J. Soileau, and E. W. Van Stryland, "Simple analysis and geometric optimization of a passive optical limiter based on internal self-interaction," SPIE Vol. 1105 pp. 146-153, 1989
4. M. Sheik-Bahae, A. A. Said, T. H. Wei, D. J. Hagan, and E. W. Van Stryland, "Sensitive measurement of optical nonlinearities using a single beam," IEEE J. Quantum Electronics, Vol. 26, No. 4, pp. 760-769, April 1990.
5. J. Rodriguez, A. Siahamakoun, G. Salamo, M. J. Miller, W. W. Clark III, G. L. Wood, E. J. Sharp, and R. R. Neurgaonkar, "BSKNN as a self-pumped phase conjugator," Applied Optics, Vol. 26, pp. 1732, 1987.
6. M. Sheik-Bahae, A. A. Said, T. H. Wei, D. J. Hagan, M. J. Soileau, and E. W. Van Stryland, "Nonlinear refraction and optical limiting in thick media," Opt. Eng., Vol.30, No. 8, pp. 1228-1235, August 1991.
7. B. K. Bairamov, B. P. Zakharchenya, and Z. M. Khashkhozhev, "Self-focusing of argon laser radiation in $Bi_{12}SIO_{20}$ crystals," Sov. Physics-Solid State, Vol 14, pp. 2357-2362, 1973.
8. P. P. Banerjee, R. M. Misra, and M. Maghraoui, "Theoretical and experimental studies of propagation of beams through a finite sample of a cubically nonlinear material," J. Opt. Soc. Am. B, Vol 8, No. 5, pp. 1072-1080, May 1991.
9. Q. W. Song, C. Zhang, P. Talbot, "Anisotropic light-induced scattering and "position dispersion' in $KNbO_3$:Fe crystal," Opt. Comm., Vol. 98, pp. 269-273, 1993.
10. H. J. Zhang, J. H. Dia, P. Y. Wang, and L. A. Wu, "Self-focusing and self trapping in new types of kerr media with large nonlinearities," Opt. Lett., Vol. 14, No. 13, pp. 695, 1989.
11. S. D. Durbin, S. M. Arakelian, and Y. R. Shen, "Laser-induced diffraction rings from a nematic-liquid-crystal film," Opt. Lett., Vol. 6, No. 9, pp. 411-413, September 1981.

Appendix A

MacPhase Macro for Calculating Self Phase Modulation

```
macro SPM;
var
        boolean : ok;
        longint: i, maxNum;
        real: R, rPhase,sum;
        Str255 : gaussName, lineName;
begin
        DisposeUnClose;
        FFTSetting(TRUE,TRUE,TRUE);
        ok:=FrontData(gaussName,'data');
        if(!ok)
                beep;
                exit;
        endif;
        maxNum:=50;
        lineName:='Line';
        NewData(lineName,1,maxNum,0,false);
        MoveWindow(lineName,400,400,TRUE);
        for(i,1,maxNum)
                R:=EvalNumber(i,*,1);
                rPhase:=EvalNumber(i,*,0.25);
                SimpleMath(gaussName,*,'None',R,'Ampiltude');
                SimpleMath(gaussName,*,'None',rPhase,'Phase');
                ok:=Exist('Farfield');
                if(ok)
                        DisposeData('Farfield');
                endif;
                FFT2D('Ampiltude','Phase',128,128,0,'Farfield','Farfield  Phase');
                SetROIOval('Farfield',59,59,72,72);
                Integrate('Farfield',3,'asdf');
                GetRIndex(1,sum);
                PutDataNumber(lineName,1,i,sum);
                PlotData(lineName,'Line  Plot',TRUE);
                MoveWindow('Farfield',400,200,TRUE);
                PlotData('Farfield','Color  Contour  Plot',TRUE);
                DisposeData('Ampiltude');
                DisposeData('Phase');
                DisposeData('Farfield  Phase');
        endfor;
end;
```

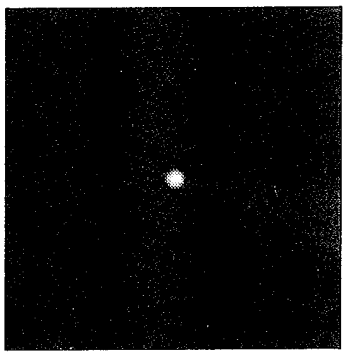

Fig. 12 Gaussian Input Laser Beam

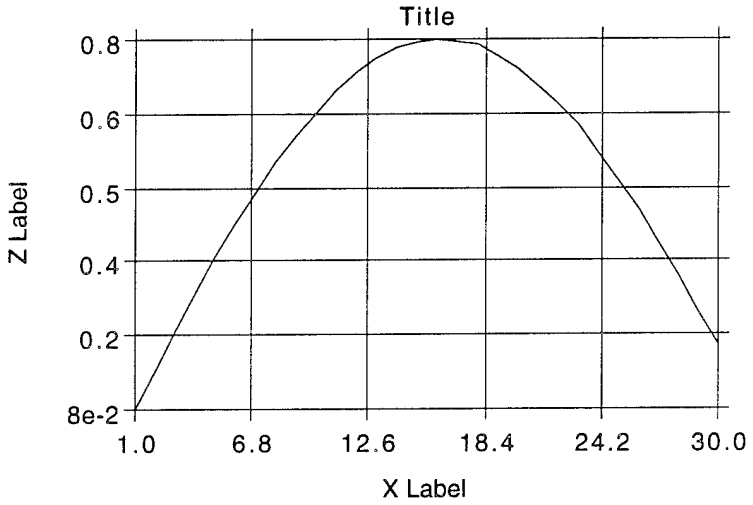

Fig. 13 Optical Limiting Influenced by SPM (normalized)

Appendix B

Matlab for SPM

```
% Plots the SPM farfield beam pattern and
% finds the power in the central half
clear
clg,hold off
load argonX,load argonY      % loads actual data
echo on
count=0;

thehalf =1253;               % previously determined from below
x=(-64:.05:63);
alpha=4.0948;                % absorption KNSBN in cm^-1
Lambda=514.5e-9;             % wavelength
d=0.05225*1e-2;      % thickness of crystal
n2=1.06e-7;                  % from Table 1
aa=(6.8e-4)^2;               % spot size of beam in crystal
phaseF=(2*pi*d*n2)/(Lambda*aa) % as in Eq. 7

% Guassian profile
sigma=1;
f=sqrt(1/(2*pi*sigma^2))*exp(-(x-4).^2/(2*sigma^2));

norm=sum(sum(f));
f=f./norm;                   % make integrated area equal to one

plot(x,f)
axis([-11  10  0  1e1])
run=1;
for k = 1:15:300,            % power in mW
      k;
      kk=k*1e-3
      count=count+1;
      xx(count)=kk;
      phase=(phaseF*kk*f);phaser=max(max(phase))/pi
      U=((kk.*f).^0.5).*exp(i.*phase);
      UU=fftshift(fft(U));IUU=(UU.*conj(UU))/1;
      plot(x,IUU),hold on
      if run == 1,       % Find the half power points
```

```
        run
        u2=IUU;
        [y,themax]=max(u2);
        y2=y/2;
        if thehalf == 0,
          for i=1:length(u2),
            if u2(i)>y2,
            u2(i)=0;
          end;
            if i>length(u2)/2,
            u2(i)=0;
          end;
        [yy,thehalf]=max(u2); % Find the half power points
       end;    % for max
      end;
      end;
      run=0;
      diff=abs(themax-thehalf)/1;
      %  Find the power contained in the center
      b(count)=sum(IUU(themax-diff:themax+diff));
end;
%pause
hold off
%plot(b')
bb=b./max(b);

% plot calculated data with actual data
plot((1e-3.*argonX),argonY),hold,plot(xx,bb),hold
```

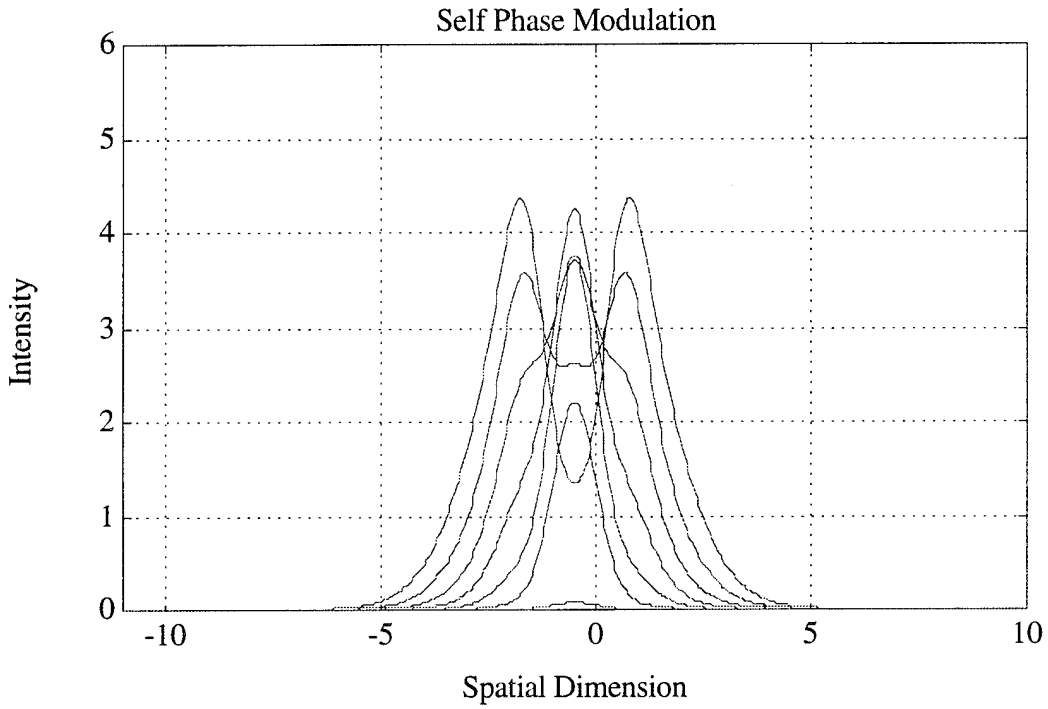
Self Phase Modulation
Intensity
Spatial Dimension
0
1
2
3
4
5
6
-10
-5
0
5
10

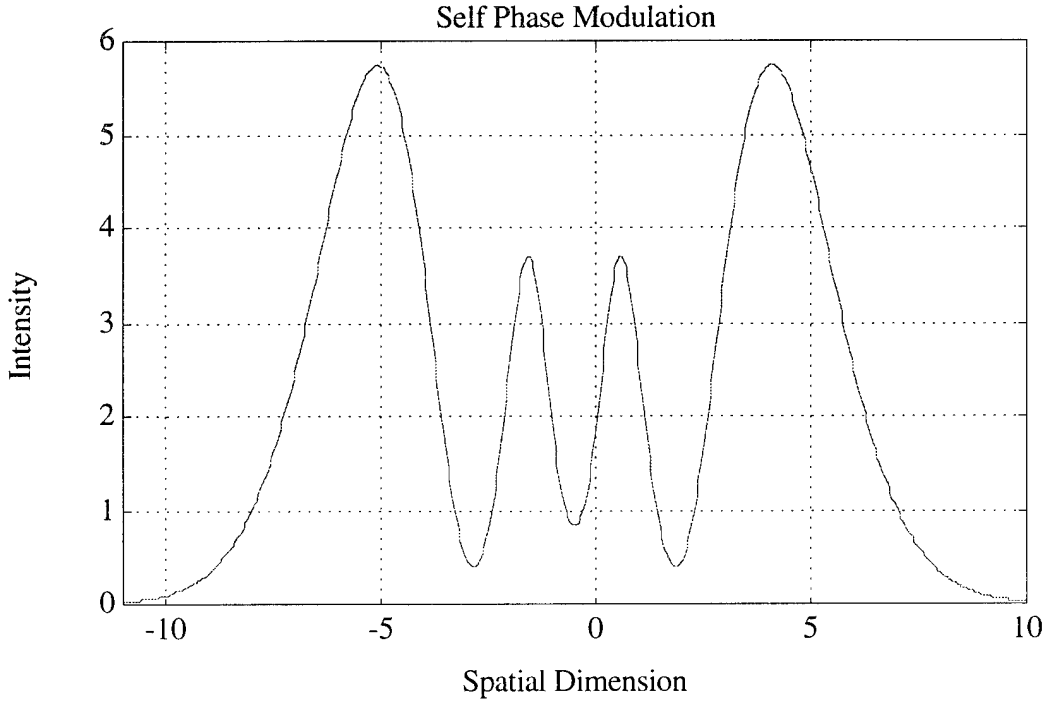
Self Phase Modulation
Intensity
Spatial Dimension
0
1
2
3
4
5
6
-10
-5
0
5
10

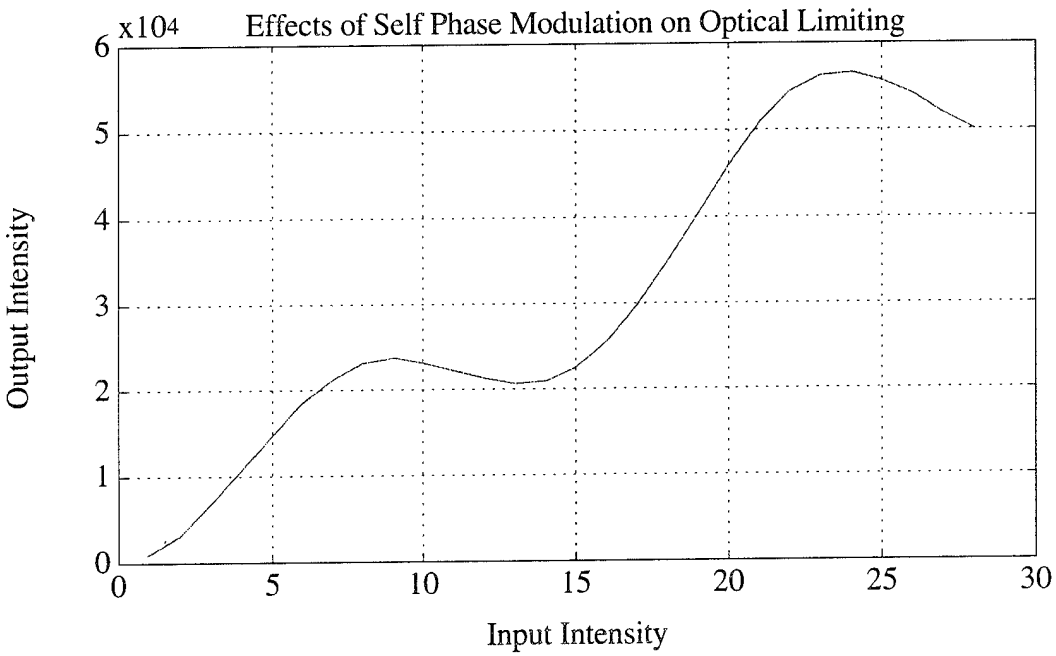


```
% SPM in 2-D
% July 28 1994 - Self Phase Modulation
clear
s=32;step=.5;
x=(-s:step:(s-step));
sigma=1;
ax=0;ay=0;                          % to offset gaussian from center
y=x';
X=ones(y)*x;
Y=y*ones(x);
R=sqrt((X-ax).^2+(Y-ay).^2) ;
f=sqrt(1/(2*pi*sigma^2))*exp(-(R).^2/(2*sigma^2));

for i = 1:1,
  num=i;
    G=num*f.*exp(i*num*f);
     B=fftshift(fft2(G))/(num*128)^2;
   IG=(B.*conj(B));
   s(i)=sum(sum(IG(61:69,61:69)));   % assuming 1/2 power
   contour(IG)
   %plot(s)
  %B=0;G=0;IG=0;
end;
```

```
contour(IG)
mesh(IG)
```

Matlab Function for calculation N_2

```
h=.5;alpha=4.0948;
lambda=476e-7;
heff=(alpha/(1-exp(-alpha*h)))
wo=2.44*lambda*.2/.004;
wo=30e-6;

f=.406*(1-.5)^.25;
Ic=2/(pi*wo^2);
k=2*pi/(lambda);
I=(Ic*.023)*1e-4
shift=(1.6)/f;
n2=(shift/(k*I))*heff          % as in Eq. 1
```

Appendix C

Matlab Function for calculation of Z-scan curve

```
% March 30 1994
hold  off,clear
step=.5;

load twox    % data from Z-scan measurements used to find n2 below
load  twoy
Power=.001;
p=max(twoy);v=min(twoy);
PV(1)=p-v;
n2=NTwo(Power,p,v)
alln(1)=n2;

% Curve fitting . . . . . .
xi=.001.*(twox(1):step:-twox(1));
si=spline(twox,twoy,xi);
c=polyfit(twox,twoy,7);
```

```
fit=polyval(c,twox);
%plot(twox,twoy,xi,si,twox,fit,xi,th);grid
%plot(twox,twoy),grid,hold  on
. . . . . .
for i = 1:2,
r= .00005+ i/2500 %+ i/3000
th=DPhaser(r+.002,(p-v),xi,1);      % DPhaser subroutine listed below
th2=DPhaser(r,(p-v),xi,0);
plot((.001.*twox),twoy,'g',xi,th2,'r',xi,th,'b'),hold  on
grid
end,pause
hold  off

load  threex              % repeated for other data values
load  threey,Power=.0025;
p=max(threey);v=min(threey);
PV(2)=p-v;
n2=NTwo(Power,p,v)
alln(2)=n2;
si=spline(threex,threey,xi);r=.000025
th=DPhaser(r+.002,(p-v),xi,1);th2=DPhaser(r,(p-v),xi,0);
plot((.001.*threex),threey,'g',xi,th2,'r',xi,th,'b')
grid,pause
hold  off

load  fourx                    % repeated for other data values
load  foury,Power=.005;
p=max(foury);v=min(foury);%'Fours',p,v
PV(3)=p-v;
n2=NTwo(Power,p,v)
alln(3)=n2;
si=spline(fourx,foury,xi);
th=DPhaser(r+.002,(p-v),xi,1);th2=DPhaser(r,(p-v),xi,0);
plot((.001.*fourx),foury,'g',xi,th2,'r',xi,th,'b')
grid,pause
hold  off

load  fivex                    % repeated for other data values
load  fivey,Power=.01;
p=max(fivey);v=min(fivey);%'Five',p,v
PV(4)=p-v;
```

```
n2=NTwo(Power,p,v)
alln(4)=n2;
si=spline(.001.*fivex,fivey,xi);r=.000015;
th=DPhaser(r+.002,(p-v),xi,1);th2=DPhaser(r,(p-v),xi,0);
th3=DPhaser(r,-(p-v),xi,0);
plot((.001.*fivex),fivey,'g',xi,th2,'r',xi,th,'r',xi,th3,'r')
averagen2=sum(alln)/4        % find average value of n2 from all
                             % inputted data
plot(alln)
AIW=74.8765;
APV=sum(PV)/4;

h=.4;alpha=6;
lambda=514e-9;
heff=(alpha/(1-exp(-alpha*h)));
wo=2.44*lambda*.2/.004;

f=.406*(1-.5)^.25;

k=2*pi/(lambda*1e2);

shift=(APV)/f;
n2=(shift/(k*AIW))*heff;
```

Matlab Subroutine DPhaser

```
function[T]=DPhase(radius,pv,z,a)
d=.44;wo=35e-6;  % Input beam radius 1.22*514.5e-9*.2/0.0036 or
.0015875
k=2*pi/(514e-9);S=.005;
if a==0,
a=6.4;%*(1-S)^(.35)
else
a=1;
end
zo=(k*wo^2)/2;DD=d/zo;
Delta=pv/(0.406*(1-.5)^(0.25)); % Change sign here for (de)focus
x=(z)./zo;
w=(wo^2)*((DD^2)*(1-(2*Delta*(DD-x).*x)./(a*DD*(1+x.^2).^2)).^2
+(1-(2*Delta*(DD-x))./(a*(1+x.^2).^2)).^2);      % as in Eq. 5
```

```
norm=(wo^2)*((DD^2)  +(1-(2*Delta*DD)./a).^2);

%w=w./norm;     % w is already squared
%  T=(1-exp(-2*(radius^2)./(w)))/(.5);          % as in Eq.4
TT=(1-exp(-2*(radius^2)./(norm)))/(.5);
T=T./mean(T);
%hold  off,plot(x,T),pause,subplot(211),plot(x,T),grid
%subplot(212),plot(x,T),grid,pause,subplot(111)
```

Rome Laboratory

Customer Satisfaction Survey

RL-TR-_____

Please complete this survey, and mail to RL/IMPS, 26 Electronic Pky, Griffiss AFB NY 13441-4514. Your assessment and feedback regarding this technical report will allow Rome Laboratory to have a vehicle to continuously improve our methods of research, publication, and customer satisfaction. Your assistance is greatly appreciated.
Thank You

_____

_____

Organization Name:_____(Optional)

Organization POC: _____(Optional)

Address:_____

1. On a scale of 1 to 5 how would you rate the technology developed under this research?

5-Extremely Useful 1-Not Useful/Wasteful

Rating_____

Please use the space below to comment on your rating. Please suggest improvements. Use the back of this sheet if necessary.

2. Do any specific areas of the report stand out as exceptional?

Yes___ No_____

If yes, please identify the area(s), and comment on what aspects make them "stand out."

3. Do any specific areas of the report stand out as inferior?

Yes___ No___

If yes, please identify the area(s), and comment on what aspects make them "stand out."

4. Please utilize the space below to comment on any other aspects of the report. Comments on both technical content and reporting format are desired.

MISSION

OF

ROME LABORATORY

Mission. The mission of Rome Laboratory is to advance the science and technologies of command, control, communications and intelligence and to transition them into systems to meet customer needs. To achieve this, Rome Lab:

a. Conducts vigorous research, development and test programs in all applicable technologies;

b. Transitions technology to current and future systems to improve operational capability, readiness, and supportability;

c. Provides a full range of technical support to Air Force Materiel Command product centers and other Air Force organizations;

d. Promotes transfer of technology to the private sector;

e. Maintains leading edge technological expertise in the areas of surveillance, communications, command and control, intelligence, reliability science, electro-magnetic technology, photonics, signal processing, and computational science.

The thrust areas of technical competence include: Surveillance, Communications, Command and Control, Intelligence, Signal Processing, Computer Science and Technology, Electromagnetic Technology, Photonics and Reliability Sciences.